

## Electrosynthesis and Characterization of an Electrochromic Material from Poly(1,6-Bis(2-(3,4-Ethylenedioxy)Thienyl)Pyrene) and Its Application in Electrochromic Device

Jinsheng Zhao<sup>1,2,\*</sup>, Xinfeng Cheng<sup>1,3</sup>, Yunzhi Fu<sup>3</sup>, Chuansheng Cui<sup>1</sup>

<sup>1</sup> Shandong Key Laboratory of Chemical Energy-storage and Novel Cell Technology, Liaocheng University, 252059, Liaocheng, P. R. China

<sup>2</sup> State Key Laboratory of Electronic Thin Films and Integrated Devices, University of electronic Science and Technology of China, Chengdu, 610054, P. R. China

<sup>3</sup> Department of Materials Science and Chemical Engineering, Hainan University, 570228, Haikou, P. R. China

\*E-mail: [j.s.zhao@163.com](mailto:j.s.zhao@163.com)

Received: 20 November 2012 / Accepted: 9 December 2012 / Published: 1 January 2013

---

1,6-bis(2-(3,4-ethylenedioxy)thienyl) pyrene monomer was successfully synthesized and electropolymerized. Characterizations of the resulting polymer poly(1,6-bis(2-(3,4-ethylenedioxy)thienyl)pyrene) (PEPE) were performed by cyclic voltammetry (CV), UV-vis spectroscopy, scanning electron microscopy (SEM). The resulting polymer presents distinct electrochromic properties with five color changes from the neutral state to oxidized state. Consequently, PEPE/PEDOT device was constructed and their characteristics were examined in detail. A potential range of 0.0–1.4 V was found to be suitable for operating the PEPE/PEDOT device between brown and blue colors. This ECD reveals fast switching time, reasonable contrast, and satisfactory open circuit memory and good stability.

---

**Keywords:** Conjugated polymer; Spectroelectrochemistry; Electrochromic device; 1,6-bis(2-(3,4-ethylenedioxy)thienyl)pyrene.

### 1. INTRODUCTION

The search for new conjugated polymers for application in thin film optoelectronic devices, such as organic light-emitting diodes (OLEDs) [1], organic photovoltaics (OPVs) [2], electrochromic devices (ECDs) [3], and organic field effect transistors (OTFTs) [4], is one of the most active areas in contemporary materials science. Tremendous recent interests have focused on the design and synthesis of novel conjugated polymers in order to achieve desirable properties for commercial applications.

Tailoring the optoelectronic properties of a conjugated polymer could be achieved by specific structural changes within the polymer backbone or by the use of distinct functional groups [5–7].

Electrochromic (EC) materials, possessing unique electrochromic properties, have been widely used in the fields of displays [8], energy-saving “smart” windows [9] and memory devices [10]. Among these EC materials, poly(3,4-ethylenedioxythiophene) (PEDOT) is a class of important EC conjugated polymers because of their high stability, high electrical conductivity, relatively low bandgap, and good chemical and electrochemical properties [11]. EDOT can give rise to noncovalent intramolecular interactions with adjacent thiophenic units and thus induce self-rigidification of the  $\pi$ -conjugated system in which it is incorporated [12]. Therefore, EDOT is prior to be chosen as a substituent or co-monomer by many researchers for fine-tuning the optoelectronic properties of various conjugated backbones through structural modifications of the monomers and copolymerization [13]. Many regioregular polymers consisting of alternating biEDOT and aromatic units (phenylene, biphenylene, naphthalene or anthracene) have been reported extensively in recent years [14,15], and it has been shown that the modification in the localization and aromaticity of the main polymer conjugation chain considerably influence the optical and electrochromic properties of the polybiEDOT. More recently, it has been reported that the introduction of pyrene bridge in didecylpropylenedioxythiophene (a derivative of EDOT) polymer main chains could result in a processable neutral state yellow to navy polymer electrochrome with a specific optical band gap of 2.2 eV, which are essential for full color displays [16]. Thus, the introduction of aromatic rings into the backbone of polybiEDOT stabilizes the conjugated  $\pi$ -bonds system effectively, and renders possibilities to obtain tunable band gap electrochromic materials, which retain the easy connectivity and good optics of EDOT. Moreover, the design of symmetrical position substitutions of the aromatic rings, such as pyrene ring, can lead to polymers with minimal side reactions upon electropolymerization [17].

In light of the above considerations, a symmetrical EDOT-bis-substituted pyrene monomer 1,6-bis(2-(3,4-ethylenedioxy)thienyl)pyrene (EPE) was synthesized and electrochemically polymerized to investigate their potential applications as electrochromic material. To our knowledge, there has been no report on the successful preparation of such materials, although Zhang and coworkers [18] described the preparation of random copolymers of pyrene and EDOT effected by the electrochemical oxidation of pyrene and EDOT at different feed ratios. We report here the electrochemical synthesis of a regioregular polymer with alternating pyrene and biEDOT repeat units by the utilization of 1,6-bis(2-(3,4-ethylenedioxy)thienyl)pyrene monomers. The obtained PEPE polymer was characterized via cyclic voltammetry, SEM, and UV–vis spectra. The spectroelectrochemical and electrochromic properties of the PEPE and its dual type polymer ECDs constructed with PEDOT were also investigated in detail.

## 2. EXPERIMENTAL

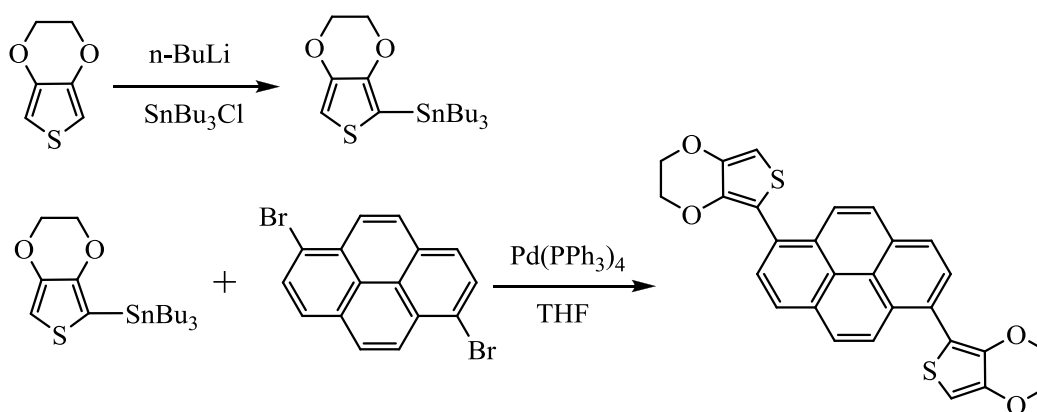
### 2.1. Materials

1,6-Dibromopyrene, 3,4-ethylenedioxythiophene (EDOT, 98%) Bis(triphenylphosphine)palladium(II) dichloride were all purchased from Aldrich Chemical and used as received. Commercial high-

performance liquid chromatography grade acetonitrile (ACN, Tedia Company, INC., USA), poly(methyl methacrylate) (PMMA, Shanghai Chemical Reagent Company), dichloromethane (DCM, Shanghai Chemical Reagent Company), propylene carbonate (PC, Shanghai Chemical Reagent Company) and lithium perchlorate ( $\text{LiClO}_4$ , Shanghai Chemical Reagent Company, 99.9%) were used directly without further purification. Sodium perchlorate ( $\text{NaClO}_4$ , Shanghai Chemical Reagent Company, 98%) was dried in a vacuum at 60 °C for 24 h before use. Other reagents were all used as received without further treatment. Indium-tin-oxide-coated (ITO) glass (sheet resistance :  $< 10 \Omega \square^{-1}$ , purchased from Shenzhen CSG Display Technologies, China) was successively washed with ethanol, acetone and deionized water in an ultrasonic bath and then dried by a constant stream of  $\text{N}_2$ .

## 2.2. Synthesis of 1,6-bis(2-(3,4-ethylenedioxy)thienyl)pyrene (EPE)

EPE was synthesized via Stille cross coupling reaction. The synthetic route of EPE is shown in Scheme 1. The precursor 2-(tri-n-butylstannyl)-3,4-ethylenedioxythiophene was prepared by a reaction between EDOT and tributyltin chloride in the presence of n-BuLi in dry THF according to literature method [19]. 1,6-Dibromopyrene and 2-(tri-n-butylstannyl)-3,4-ethylenedioxythiophene were dissolved in dry THF. The solution was purged with nitrogen for 30 min and Bis(triphenylphosphine)palladium(II) dichloride was added at room temperature. The mixture was refluxed over night under nitrogen atmosphere. The crude mixture was chromatographed on silica gel by eluting with hexane: ethyl acetate (4:1, v/v) to give EPE as yellow solid (47%).  $^1\text{H}$  NMR ( $\text{CDCl}_3$ , 400 M Hz, ppm):  $\delta = 4.26\text{--}4.32$  (m, 8H), 6.57 (s, 2H), 8.08 (dd, 4H), 8.19 (d, 2H), 8.30 (d, 2H). Elemental analysis for:  $\text{C}_{28}\text{H}_{18}\text{O}_4\text{S}_2$ , Calc. C, 69.71; H, 3.73; S, 13.28. Found: C, 69.51; H, 3.79; S, 13.32.



**Scheme 1.** The synthetic route of the monomer EPE

## 2.3. Instrumentation

Elemental analyses were determined by a Thermo Finnigan Flash EA 1112, CHNS-O elemental analyses instrument. Scanning electron microscopy (SEM) measurements were taken by using a Hitachi SU-70 thermionic field emission SEM. Cyclic voltammetry was carried out on CHI

760 C electrochemical workstation using three-electrode system. UV–vis spectra were measured on a Perkin-Elmer Lambda 900 UV–vis–near-infrared spectrophotometer. Digital photographs of the polymer films and device cell were taken by a Canon Power Shot A3000 IS digital camera.

#### 2.4. Electrochemical and spectroelectrochemical measurements

Electrochemical synthesis and experiments were performed in a one-compartment cell with a CHI 760 C Electrochemical Analyzer under the control of a computer, employing a platinum wire with a diameter of 0.5 mm as working electrode, a platinum ring as counter electrode, and a Ag wire (0.03 V vs. SCE. [20]) as pseudo reference electrode. All electrochemical polymerization and CV tests were performed in ACN/DCM (1:1, v:v) solution containing 0.2 M NaClO<sub>4</sub> as a supporting electrolyte at room temperature under nitrogen atmosphere.

Spectroelectrochemical data were recorded on Perkin-Elmer Lambda 900 UV–vis–near-infrared spectrophotometer connected to a computer. A three-electrode cell assembly was used where the working electrode was an ITO glass, the counter electrode was a stainless steel wire, and an Ag wire was used as the pseudo reference electrode. The polymer films that were used for spectroelectrochemistry were prepared by potentiostatically depositing the polymer onto the ITO electrode (the active area: 0.9 cm × 2.1 cm). The measurements were carried out in ACN/DCM (1:1, v:v) solution containing 0.2 M NaClO<sub>4</sub>. Moreover, the thickness of the polymer films grown potentiostatically on the ITO electrode was controlled by the total charge passed through the cell.

#### 2.5. Construction of ECDs

Both anodically (PEPE) and cathodically (PEDOT) coloring polymers were electrochemically deposited onto the ITO-coated glass from a 0.2 M NaClO<sub>4</sub>/ACN/DCM with the same polymerization charge ( $2.3 \times 10^{-2}$  C). The redox sites of these polymer films were matched by stepping the potentials between their extreme states. ECDs were built by arranging two electrochromic polymer films (one doped, the other neutral) facing each other and separated by gel electrolyte. The gel electrolyte was prepared according to literature [21].

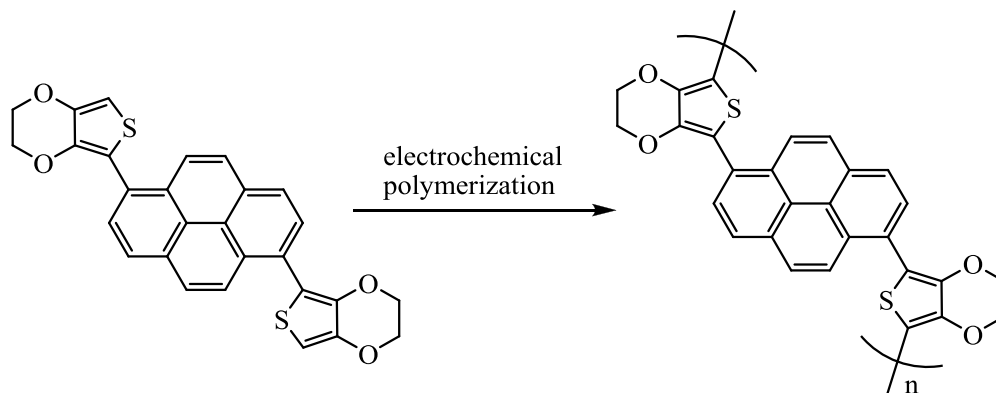
### 3. RESULTS AND DISCUSSION

#### 3.1. Electrochemical polymerization and characterization of PEPE films

##### 3.1.1. Electrochemical polymerization

Electrochemical polymerization process was carried out in a reaction medium containing 0.005 M EPE monomer and 0.2 M NaClO<sub>4</sub> in acetonitrile-dichloromethane (1:1; v:v) via repetitive cycling at a scan rate of 100 mV s<sup>-1</sup>. The electrochemical polymerization of EPE monomer is illustrated in Scheme 2. The electroactive polymer was directly coated onto the working electrode (platinum wire).

As seen in Fig. 1, the polymer film obtained by repetitive cycling at a potential between 0 and 1.3 V (potentiodynamic method) exhibited two reversible waves located at 0.70–0.58 V and 0.89–0.85 V, which were ascribed to the EDOT and pyrene units, respectively. The increased current density after each successive cycle clearly indicated the formation of a homogeneous PEPE film deposited onto the surface of the working electrode [22].



**Scheme 2.** The electrochemical polymerization of EPE monomer.

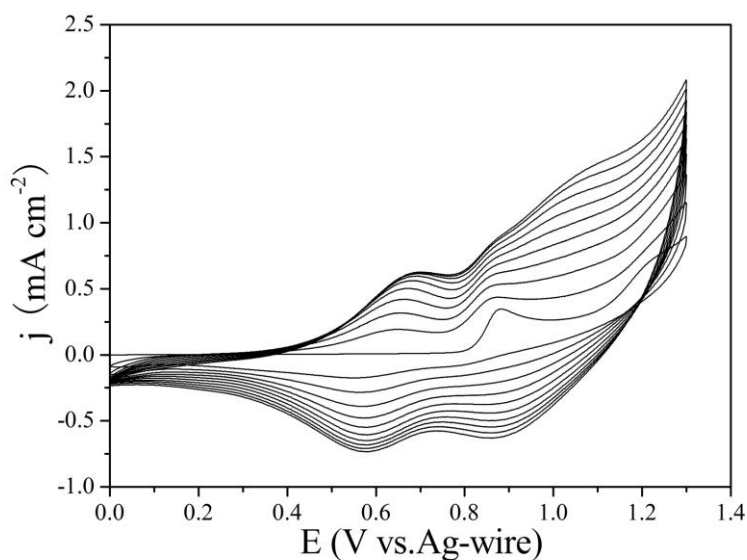


**Figure 1.** Cyclic voltammogram curves of 0.005 M EPE in 0.2 M NaClO<sub>4</sub>/ACN/DCM solution at a scan rate of 100 mV s<sup>-1</sup>. *j* denotes the current density.

### 3.1.2. Polymer electrochemistry

Cyclic voltammetry was used to probe the accessible redox states in the PEPE film as deposited by the repeated scanning method. Fig. 2 shows the CV curves of the PEPE film at different scan rates between 25 and 300 mV s<sup>-1</sup> in monomer free ACN/DCM (1:1; v:v) containing 0.2 M NaClO<sub>4</sub>. As can

be seen from Fig. 2, bottom inset, the PEPE film exhibited two pairs of redox peaks located at 0.66–0.57 V and 0.98–0.89 V, respectively. Compare to the polypyrene behavior [23], the polymer PEPE displays good redoxactivity, which is in accordance with the structurally similar didecylpropylenedioxythiophene bis-substituted pyrene derivatives reported in literature [16]. The scan rate dependence of the anodic and cathodic peak current densities was studied in a monomer-free electrolyte solution (Fig. 2, top inset). A linear relationship was found between the peak current and the scan rate. This relationship indicates that the electroactive polymer film was well adhered to the electrode surface and the redox processes were non-diffusional.

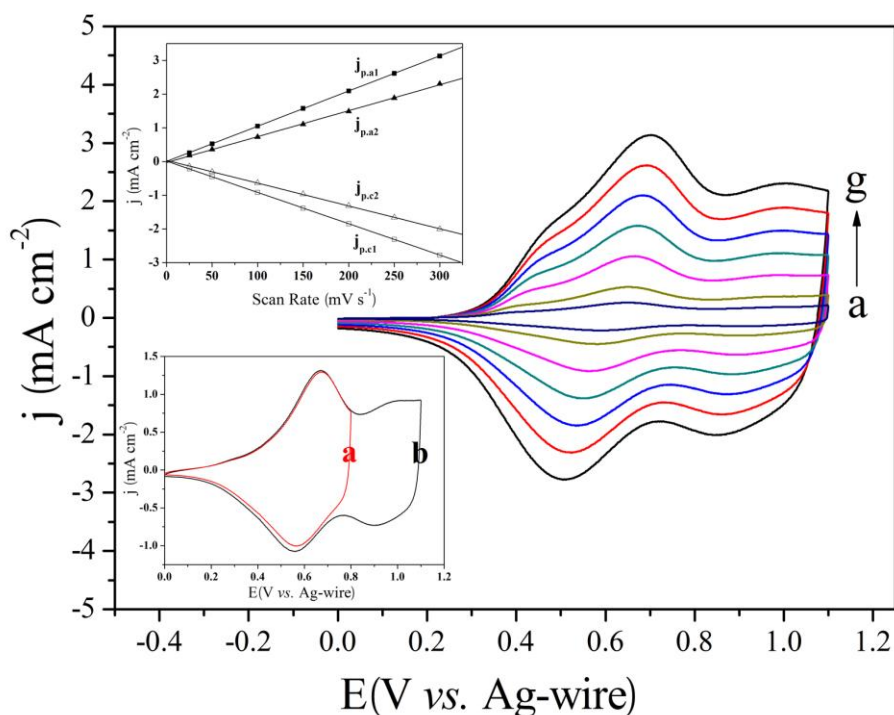


**Figure 2.** Cyclic voltammetry of PEPE film in the monomer-free 0.2 M NaClO<sub>4</sub>/ACN/DCM solution at different scan rates: (a) 25, (b) 50, (c) 100, (d) 150, (e) 200, (f) 250, (g) 300 mV/s. Top inset: Graph of the scan rate dependence of the anodic ( $j_{p,a1}$ ,  $j_{p,a2}$ ) and cathodic ( $j_{p,c1}$ ,  $j_{p,c2}$ ) peak current densities. Bottom inset: Cyclic voltammogram of PEPE showing (a) first redox couple, (b) second redox couple (waveclipping).

### 3.1.3. Morphology

The morphology of PEPE film was investigated by scanning electron microscopy (SEM). The PEPE film was prepared by constant potential electrolysis from the solution of 0.2 M NaClO<sub>4</sub>/ACN/DCM containing 0.005 M monomer on ITO electrode and dedoped before characterization. As shown in Fig. 3, the PEPE film displays a porous structure with accumulations of small granules. Such porous structure is great helpful in the movement of counterions into and out of the polymer film during doping and dedoping, in good agreement with its good redoxactivity.

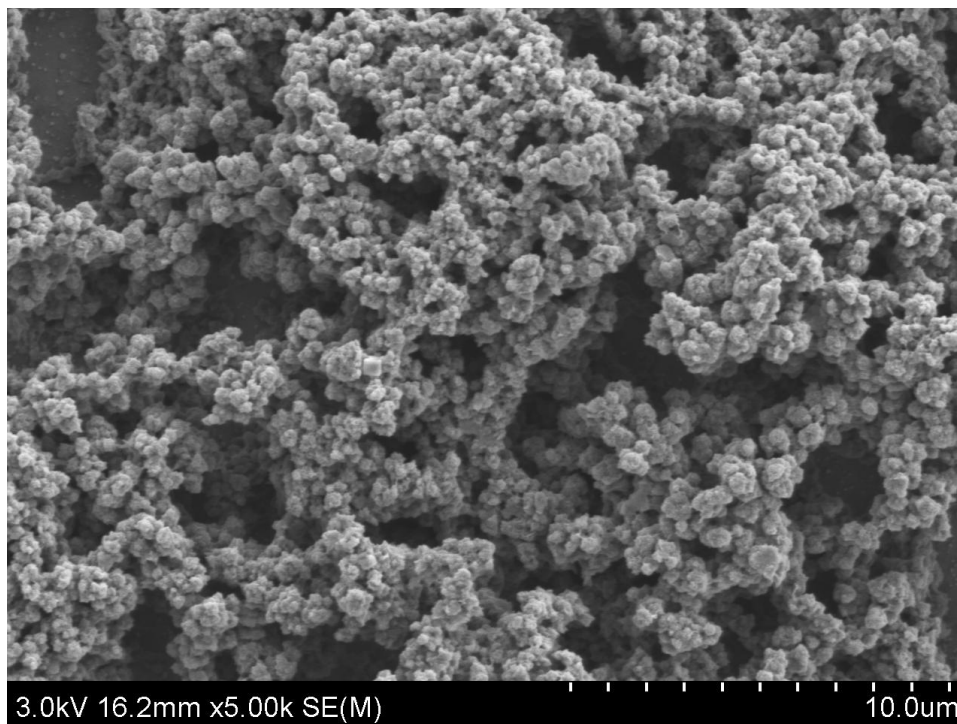


**Figure 3.** SEM image of dedoped PEPE film.

#### 3.1.4. Optical properties of EPE monomer and PEPE film

The UV–vis spectra of EPE monomer in DCM and PEPE film deposited on ITO electrode are shown in Fig. 4. As seen in Fig. 4, the absorption maximum ( $\lambda_{\max}$ ) of the monomer EPE and the neutral state PEPE are centered at 379 and 467 nm, respectively. The difference between the  $\lambda_{\max}$  corresponding to the monomer and the corresponding polymer for EPE, which is about 88 nm, is owing to the increased conjugation length in the polymer. Moreover, the optical band gap ( $E_g$ ) of monomer and polymer were calculated from their low energy absorption edges ( $\lambda_{\text{onset}}$ ) ( $E_g = 1240/\lambda_{\text{onset}}$ ). The  $E_g$  of the PEPE film was calculated as 2.22 eV, which was lower than that of monomer EPE (2.89 eV), clearly due to the extended conjugation length.

The optical parameters of EPE and PEPE are summarized in Table 1 together with the corresponding data for pyrene, 2,2'-bis-(3,4-ethylenedioxy)thiophene (biEDOT) [24], poly(pyrene) (PPy) and poly(3,4-ethylenedioxythiophene) (PEDOT) [25] for comparison. As shown in Table 1, the  $\lambda_{\max}$  of EPE monomer was red shifted by approximately 29 nm to 43 nm compare to that of biEDOT (350 nm) and pyrene (336 nm) due to the extended degree of conjugation ( $\pi$ – $\pi^*$  bonding system) by the introduction of pyrene bridge into the head-to-head  $\alpha$ – $\alpha'$  coupling of EDOT unit. While the  $E_g$  of polymer PEPE was lower than that of polypyrene (2.67 eV) but higher than that of PEDOT (1.65 eV) due to the different conjugation length along the polymer backbone. In addition, Table 1 also clearly summarizes the onset oxidation potential ( $E_{\text{onset}}$ ) and HOMO/LUMO levels of the monomers and polymers. HOMO energy levels of them were calculated by using the formula  $E_{\text{HOMO}} = -e(E_{\text{onset}} + 4.4)$  ( $E_{\text{onset}}$  vs. SCE) and LUMO energy levels ( $E_{\text{LUMO}}$ ) of them were calculated by the subtraction of the optical band gap from the HOMO levels [26].

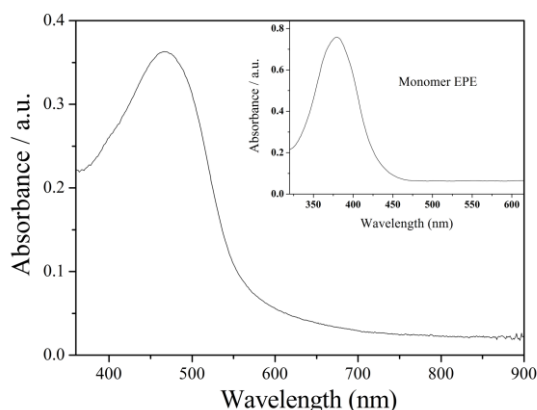


**Figure 4.** UV-vis spectrum of PEPE film deposited on ITO electrode at the dedoped state. Inset: absorption spectrum of EPE monomer dissolved in  $\text{CH}_2\text{Cl}_2$ .

**Table 1.** The onset oxidation potential ( $E_{\text{onset}}$ ), maximum absorption wavelength ( $\lambda_{\text{max}}$ ), HOMO and LUMO energy levels and optical band gap ( $E_g$ ) of pyrene, biEDOT, EPE, PPy, PEDOT and PEPE.

Compounds	$E_{\text{onset}}$ , vs.(Ag-wire) (V)	$\lambda_{\text{max}}$ (nm)	$E_g^a$ (eV)	HOMO (eV)	LUMO <sup>b</sup> (eV)
pyrene	1.13	320, 336	3.63	-5.56	-1.93
biEDOT <sup>c</sup>		330, 350			
EPE	0.81	379	2.89	-5.24	-2.35
PPy	0.96	357	2.67	-5.39	-2.72
PEDOT <sup>d</sup>	-0.64	595	1.65	-3.84	-2.19
PEPE	0.31	467	2.22	-4.74	-2.52

<sup>a</sup> Calculated from the low energy absorption edge:  $E_g = 1240/\lambda_{\text{onset}}$ .

<sup>b</sup> Calculated by the subtraction of the optical band gap from the HOMO level.

<sup>c</sup> Data were taken from Ref. [24].

<sup>d</sup> Data were taken from Ref. [25].

### 3.2. Electrochromic properties of PEPE film

#### 3.2.1. Spectroelectrochemical properties of PEPE film

Spectroelectrochemistry can be used as an efficient method to investigate the optical properties of an electrochromic conducting polymer upon potential change, which also provides information about the electronic structure of the conducting polymer [27]. The PEPE film was electrodeposited onto ITO electrode (the active area was  $0.9 \text{ cm} \times 2.1 \text{ cm}$ ) with the polymerization charge of  $2.6 \times 10^{-2} \text{ C}$ . It was switched between 0 and 1.1 V in monomer-free 0.2 M  $\text{NaClO}_4/\text{ACN}/\text{DCM}$  solution in order to obtain the in situ UV-vis spectra (Fig. 5). At the neutral state, the polymer film exhibited an absorption peak at 467 nm due to the  $\pi-\pi^*$  transition. Upon increase of the applied potential, the intensity of the PEPE  $\pi-\pi^*$  electron transition absorption decreased while two charge carrier

absorption bands located at around 720 nm and longer than 850 nm increased dramatically. The appearance of charge carrier bands could be attributed to the evolution of polaron and bipolaron bands.

Furthermore, the observed UV-vis absorption changes in the film of PEPE at various potentials are fully reversible and are associated with distinct color changes. From the inset shown in Fig. 6, it can be seen that the PEPE film switches from brown in the neutral state (0 V) which passes to a grayish brown at 0.6 V. With the increase of potential, the polymer film turns into grayish green (0.7 V), grayish blue (0.8 V), and then to steel blue color at full doped state (1.1 V), respectively. This multicolor property possesses significant potential applications in smart windows or displays.

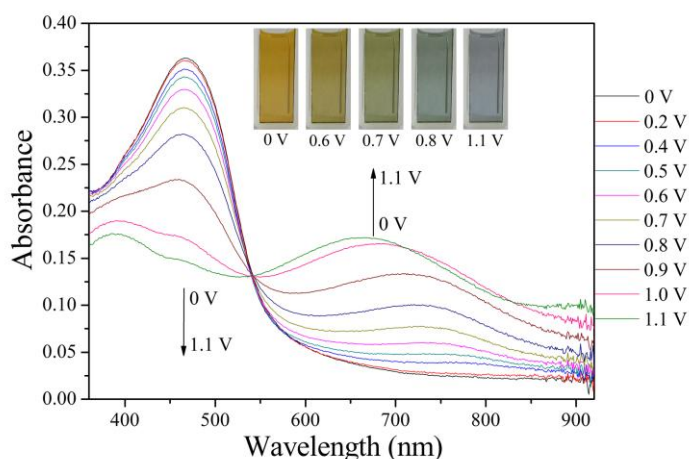


**Figure 5.** Spectroelectrochemical spectra of the PEPE film on ITO electrode as applied potentials between 0 V and 1.1 V in monomer-free 0.2 M NaClO<sub>4</sub>/ACN/DCM solution. Inset: colors of polymer film at different applied potentials.

### 3.2.2. Electrochromic switching of PEPE film in solution

For electrochromic switching studies, the polymer film was potentiostatically deposited onto ITO-coated glass (active area: 0.9 cm × 2.1 cm) with the polymerization charge of  $2.6 \times 10^{-2}$  C in the same manner as described above, and the film was subsequently stepped between its neutral (0 V) and oxidized (1.1 V) state in 3 s intervals in 0.2 M NaClO<sub>4</sub>/ACN/DCM solution. While the film was switched, the transmittance at 710 nm was monitored as a function of time with UV-vis-NIR spectroscopy. One important characteristic of electrochromic materials is the optical contrast ( $\Delta T\%$ ), which can be defined as the transmittance difference between the redox states. As shown in Fig. 6, the optical contrast of the PEPE at 710 nm was found to be 20.6%. Response time, one of the most important characteristics of electrochromic materials, was calculated at 95% of the full switch because of the difficulty in perceiving any further color changes with the naked eye beyond this point [28]. The optical response time of PEPE were found to be 0.47 s from the oxidized to the reduced state and 1.28 s from the reduced to the oxidized state, which is also faster than that of the structurally similar poly(1,6-bis(2-(didecylpropylenedioxy)thienyl)pyrene) reported in literature [16]. Stepping from the oxidized to the reduced state is inherently faster than stepping from the reduced to the oxidized state.

This can be attributed to the ease of charge transport in the conducting film as it is reduced. The acceptable optical contrast and reasonable response time make this polymer a promising material for electrochromic devices.

The coloration efficiency (CE) is also an important characteristic for the electrochromic materials. It is defined as the change in the optical density ( $\Delta OD$ ) for the charge consumed per unit electrode area ( $\Delta Q$ ) [29]. The corresponding equations are given below:

$$\Delta OD = \lg\left(\frac{T_b}{T_c}\right) \quad \text{and} \quad \eta = \frac{\Delta OD}{\Delta Q}$$

where  $T_b$  and  $T_c$  are the transmittances before and after coloration, respectively, and  $\eta$  denotes the coloration efficiency (CE). CE of PEPE film was measured as  $72.7 \text{ cm}^2 \text{ C}^{-1}$  (at 710 nm) at full doped state, which had reasonable coloration efficiency.

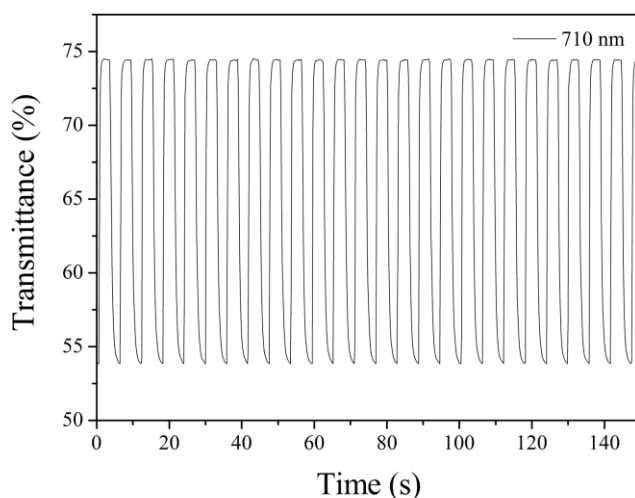


**Figure 6.** Spectroelectrochemical spectra of the PEPE film on ITO electrode as applied potentials between 0 V and 1.1 V in monomer-free 0.2 M  $\text{NaClO}_4/\text{ACN}/\text{DCM}$  solution. Inset: colors of polymer film at different applied potentials.

### 3.3. Spectroelectrochemistry of electrochromic devices (ECDs)

#### 3.3.1. Spectroelectrochemical properties of ECDs

In order to investigate the electrochromic performance of the PEPE polymer in electrochromic devices, dual type complementary colored ECDs consisting of PEPE and PEDOT were constructed. The optoelectronic behavior of the ECDs were investigated by the UV–vis spectrophotometer as a function of applied potential. Fig. 7 shows the spectroelectrochemistry study of PEPE/PEDOT ECD between 0 V and 1.4 V. At 0 V, the device revealed a maximum absorption at 464 nm and its color was brown. At this stage, the PEPE polymer was in its neutral state revealing brown and PEDOT was in its oxidized form (highly transparent blue) revealing on significant absorption at the visible region

and hence the color of the ECD was brown. As the applied potential increased, simultaneous reduction of the PEDOT and oxidation of PEPE layers, which were signified with the decrease in the intensity of the peak at 464 nm and increase in the intensity of the peak at 630 nm, were observed. At 1.4 V as the spectral signatures of both layers become dominant, the color of the device turned into blue, indicating that the PEDOT and PEPE were in their fully neutral and oxidized states, respectively.

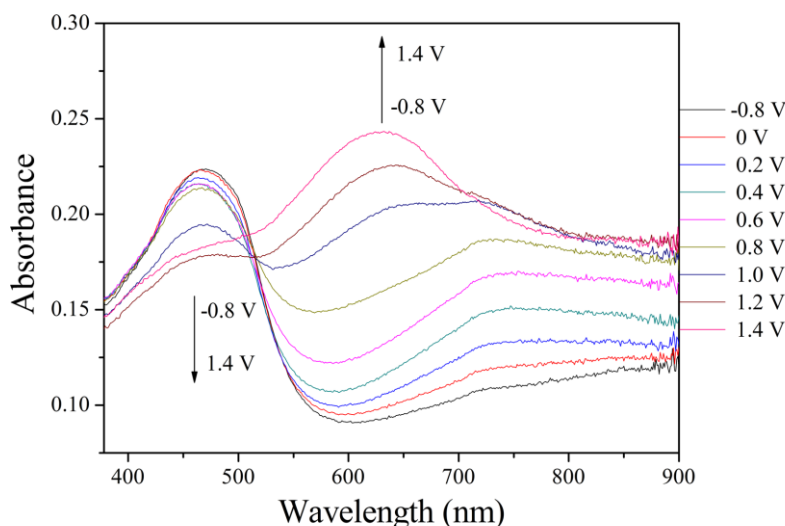


**Figure 7.** Spectroelectrochemical spectra of the PEPE/PEDOT device at various applied potentials from  $-0.8$  to  $1.4$  V.

### 3.3.2. Switching of ECD

The most important property of an ECD is the switching time and its optical contrast. Chronoabsorptometry technique was used to perform the measurements. The wavelength of the measurement depending on the optical contrast was found to be  $630$  nm and the switching potentials were applied from  $0$  V to  $1.4$  V at regular intervals of  $2$  s (Fig. 8). The optical contrast ( $\% \Delta T$ ) was found to be  $27\%$ . The response time was determined to be  $0.90$  s at  $95\%$  of the maximum transmittance difference from the neutral state to oxidized state and  $0.23$  s from the oxidized state to the neutral state. The device also has a high coloration efficiency (CE), which was calculated to be  $226.8$   $\text{cm}^2 \text{C}^{-1}$  at  $630$  nm.

### 3.3.3. Open circuit memory of ECD

The open circuit memory is an important characteristic because it is directly related to its application and energy consumption during the use of ECDs. It is defined as the time period in which the device retains its color under open circuit conditions [30]. In order to evaluate the open-circuit memory characteristic of the constructed ECD sandwich cell, the device was monitored at  $630$  nm as a

function of time at  $-0.8$  V and  $1.4$  V by applying the potential for 1 s for each 200 s time interval. As depicted in Fig. 9, in brown colored state, the device showed a true permanent memory effect since there was almost no transmittance change under the applied potential ( $-0.8$  V) or open circuit conditions. In blue colored state, the device was rather less stable in terms of color persistence, however, this matter can be overcome by applying current pulses to freshen the fully colored states.

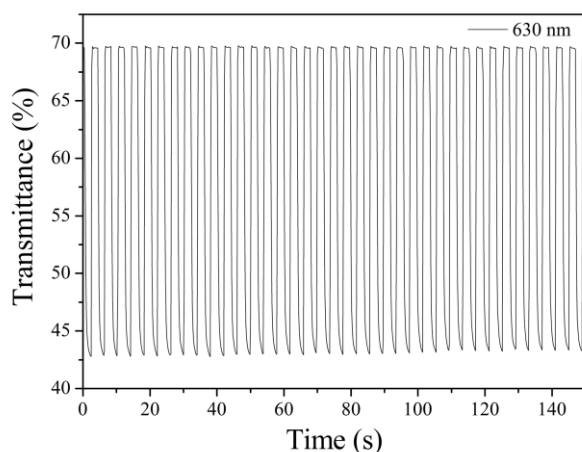


**Figure 8.** Electrochromic switching, optical transmittance change monitored at 630 nm for the PEPE/PEDOT device between  $-0.8$  V and  $1.4$  V with a residence time of 2 s.

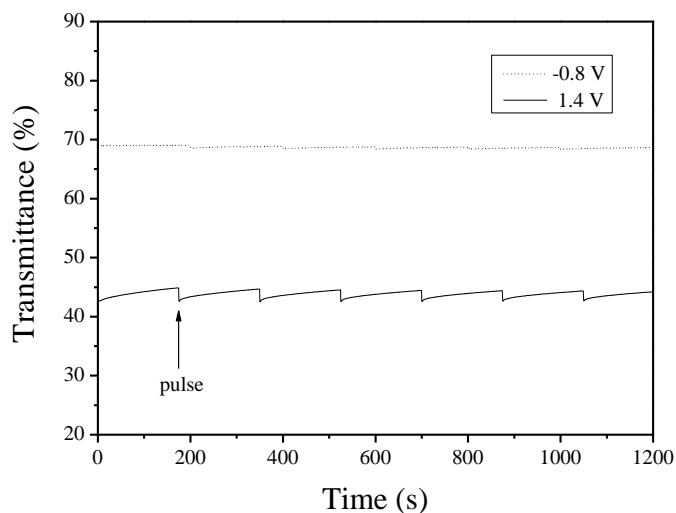


**Figure 9.** Open circuit stability of the PEPE/PEDOT device monitored at 630 nm.

#### 3.3.4. Stability of ECD

Electrochromic stability is associated with electrochemical stability since the degradation of the active redox couple results in the loss of electrochromic contrast. The stability of the PEPE/PEDOT was monitored by cyclic voltammetry of the applied potential between  $-0.8$  and  $1.4$  V with  $500$   $\text{mV s}^{-1}$

(Fig. 10). The ECD revealed 9% loss of its electroactivity accompanied by unperturbed color change from bleached to colored state after 1000 cycles, indicating that this device has good redox stability.

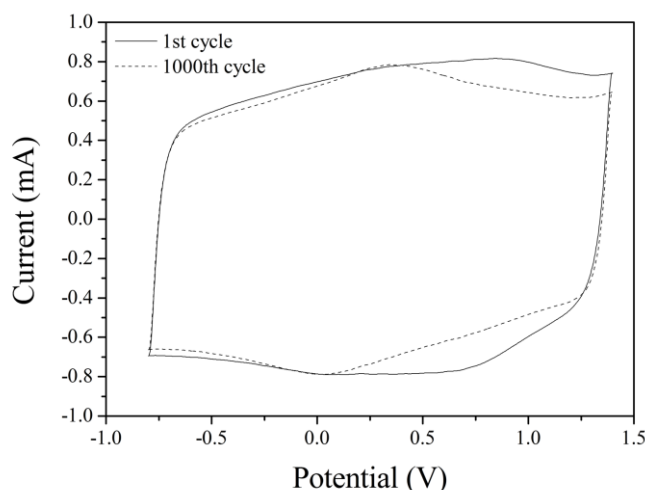


**Figure 10.** Cyclic voltammogram of the PEPE/PEDOT device as a function of repeated scans with  $500 \text{ mV s}^{-1}$ .

#### 4. CONCLUSIONS

1,6-bis(2-(3,4-ethylenedioxy)thienyl)pyrene monomer was synthesized by Stille coupling reaction and then its polymer was successfully synthesized by electrochemical oxidation of the monomer in  $0.2 \text{ M NaClO}_4/\text{ACN}/\text{DCM}$  solution. UV-vis absorption analyses show that the PEPE polymer reveals a reduced optical bandgap ( $2.22 \text{ eV}$ ) compared to polypyrene ( $2.67 \text{ eV}$ ), indicating a greater  $\pi$ -delocalization along the polymer backbone. Spectroelectrochemistry reveals that PEPE film has distinct electrochromic properties and shows five different colors (brown, grayish brown, grayish green, grayish blue and steel blue) under various potentials. Maximum contrast ( $\Delta T\%$ ) and response time of the PEPE film were measured as  $20.6\%$  and  $1.28 \text{ s}$  at  $710 \text{ nm}$ . The PEPE/PEDOT ECD was also constructed and characterized. Electrochromic switching study results show that optical contrast ( $\Delta T\%$ ) and response time are  $27\%$  and  $0.9 \text{ s}$  at  $630 \text{ nm}$ , respectively. The CE of the ECD was calculated to be  $226.8 \text{ cm}^2 \text{ C}^{-1}$ . This ECD also exhibits good redox stability with unperturbed color change from brown to blue. These properties make PEPE a good candidate for commercial applications.

#### ACKNOWLEDGEMENTS

The work was financially supported by the Open Foundation of the State key Laboratory of Electronic Thin Films and Integrated Devices, University of electronic Science and Technology of China (KFJJ201114) and Taishan Scholarship of Shandong Province.

## References

1. H. Siringhaus, M. Bird, N. Zhao, *Adv. Mater.* 22 (2010) 3893–3898.
2. A.P. Zoombelt, M. Fonrodona, M.G.R. Turbiez, M.M. Wienk, R.A.J. Janssen, *J. Mater. Chem.* 19 (2009) 5336–5342.
3. P.M. Beaujuge, J.R. Reynolds, *Chem. Rev.* 110 (2010) 268–320.
4. C. Poriel, J.-J. Liang, J. Rault-Berthelot, F. Barrière, N. Cocherel, A.M.Z. Slawin, D. Horhant, G.M. Virboul, N.A. Audebrand, L. Vignau, N. Huby, L. Hirsch, G. Wantz, *Chem. Eur. J.* 13 (2007) 10055–10069.
5. C. Kitamura, S. Tanaka, Y. Yamashita, *Chem. Mater.* 8 (1996) 570–578.
6. L. Groenendaal, G. Zotti, P.-H. Aubert, S.M. Waybright, J. R. Reynolds, *Adv. Mater.* 15 (2003) 855–879.
7. S. Tarkuc, Y.A. Udum, L. Toppare, *Thin Solid Films.* 520 (2012) 2960–2965.
8. R.J. Mortimer, A.L. Dyer, J.R. Reynolds, *Displays.* 27 (2006) 2–18.
9. A. Azens, C.G. Granqvist, *J. Solid State Electrochem.* 7 (2003) 64–68.
10. S. Möller, C. Perlov, W. Jackson, C. Taussig, S.R. Forrest, *Nature.* 426 (2003) 166–169.
11. J.K. Xu, G.M. Nie, S.S. Zhang, X.J. Han, J. Hou, S.Z. Pu, *J. Mater. Sci.* 40 (2005) 2867–2873.
12. J.M. Raimundo, P. Blanchard, P. Frere, N. Mercier, I. Ledoux Rak, R. Hierle, J. Roncali, *Tetrahedron Lett.* 42 (2001) 1507–1510.
13. G. Gunbas, L. Toppare, *Chem. Commun.* 48 (2012) 1083–1101.
14. G.A. Sotzing, J.R. Reynolds, *Chem. Mater.* 8 (1996) 882–889.
15. A.M. Fraind, J.D. Tovar, *J. Phys. Chem. B.* 114 (2010) 3104–3116.
16. M. İçli-Özkut, Z. Öztaş, F. Alğı, A. Cihaner, *Org. Electron.* 12 (2011) 1505–1511.
17. B. Sankaran, M.D. Alexander Jr., L.S. Tan, *Synth. Met.* 123 (2001) 425–433.
18. C. Zhang, Y. Xu, N. Wang, C. Yu, W. Xiang, M. Ouyang, C. Ma, *Electrochim. Acta.* 55 (2009) 13–18.
19. S.S. Zhu, T.M. Swager, *J. Am. Chem. Soc.* 119 (1997) 12568–12577.
20. X.F. Cheng, J.S. Zhao, C.S. Cui, Y.Z. Fu, X.X. Zhang, *J. Electroanal. Chem.* 677–680 (2012) 24–30.
21. Y.Z. Fu, X.F. Cheng, J.S. Zhao, T.Y. Kong, C.S. Cui, X.X. Zhang, *Polym. J.* 44 (2012) 1048–1055.
22. O. Mert, E. Sahin, E. Ertas, T. Ozturk, E.A. Aydin, L. Toppare, *J. Electroanal. Chem.* 591 (2006) 53–58.
23. L.Y. Xu, J.S. Zhao, R.M. Liu, H.T. Liu, J.F. Liu, H.S. Wang, *Electrochim. Acta.* 55 (2010) 8855–8862.
24. M. Chahma, R.G. Hicks, *Can. J. Chem.* 82 (2004) 1629–1633.
25. B. Wang, J.S. Zhao, C.S. Cui, R.M. Liu, J.F. Liu, H.S. Wang, H.T. Liu, *Electrochim. Acta.* 56 (2011) 4819–4827.
26. Y.F. Li, Y. Cao, J. Gao, D.L. Wang, G. Yu, A.J. Heeger, *Synth. Met.* 99 (1999) 243–248.
27. J. Hwang, J.I. Son, Y.-B. Shim, *Sol. Energy Mater. Sol. Cells.* 94 (2010) 1286–1292.
28. A. Cihaner, F. Alğı, *Electrochim. Acta.* 54 (2008) 786–792.
29. M. Deepa, A. Awadhia, S. Bhandari, *Phys. Chem. Chem. Phys.* 11 (2009) 5674–5685.
30. P. Camurlu, L. Toppare, *J. Macromol. Sci. A.* 43 (2006) 449–458.